Electronic Supplementary Material (ESI) for Journal of Materials Chemistry A.

Supplementary Information

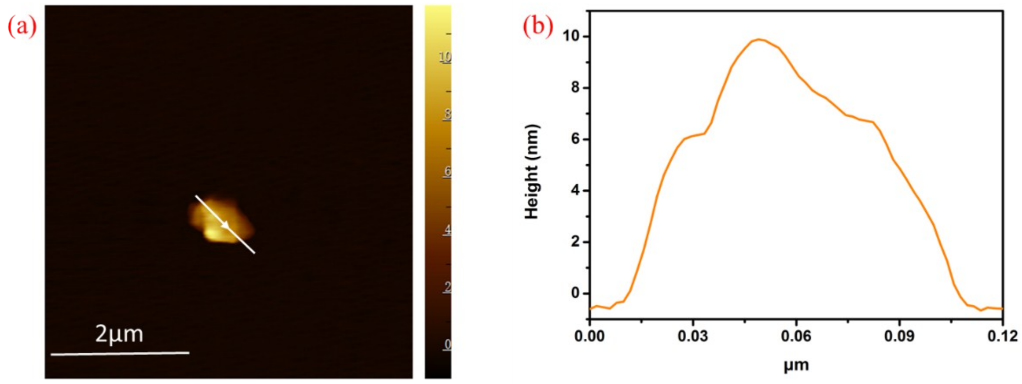

Fig. S1 (a) AFM image of the BNNSs and (b) corresponding height information.

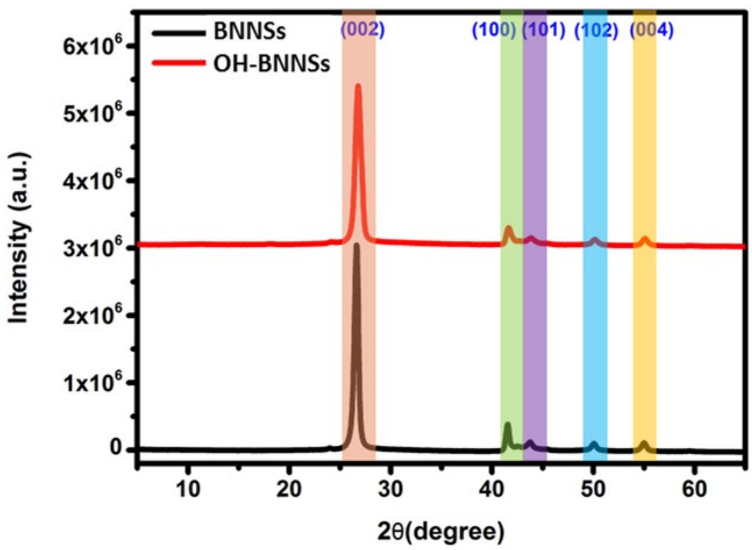

Fig. S2 The representative XRD image of BNNSs and OH-BNNSs. The peaks of BNNSs and OH-BNNSs at 2θ≈27°, 42°,44°, 55° results from the diffraction of (002), (100), (101), (102) and (004) peaks of h-BN.

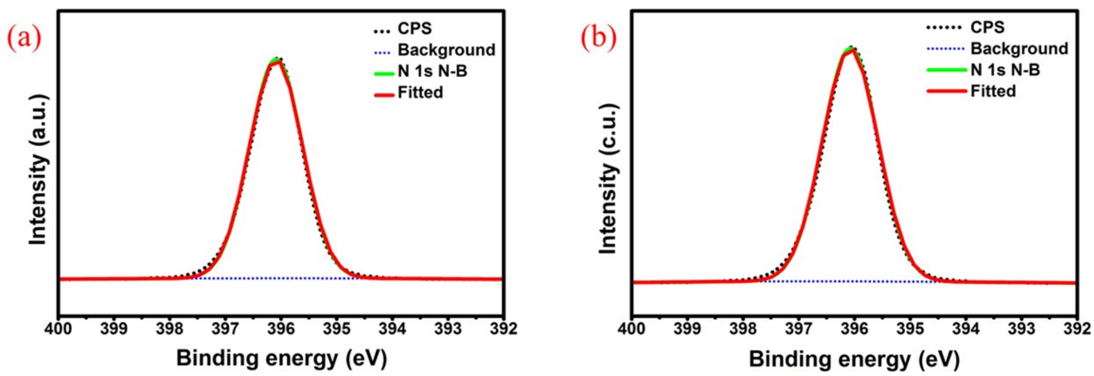

Fig. S3 N 1s spectra of (a) BNNSs and (b) OH-BNNSs, and showing that the hydroxyl groups do not graft onto N atoms.

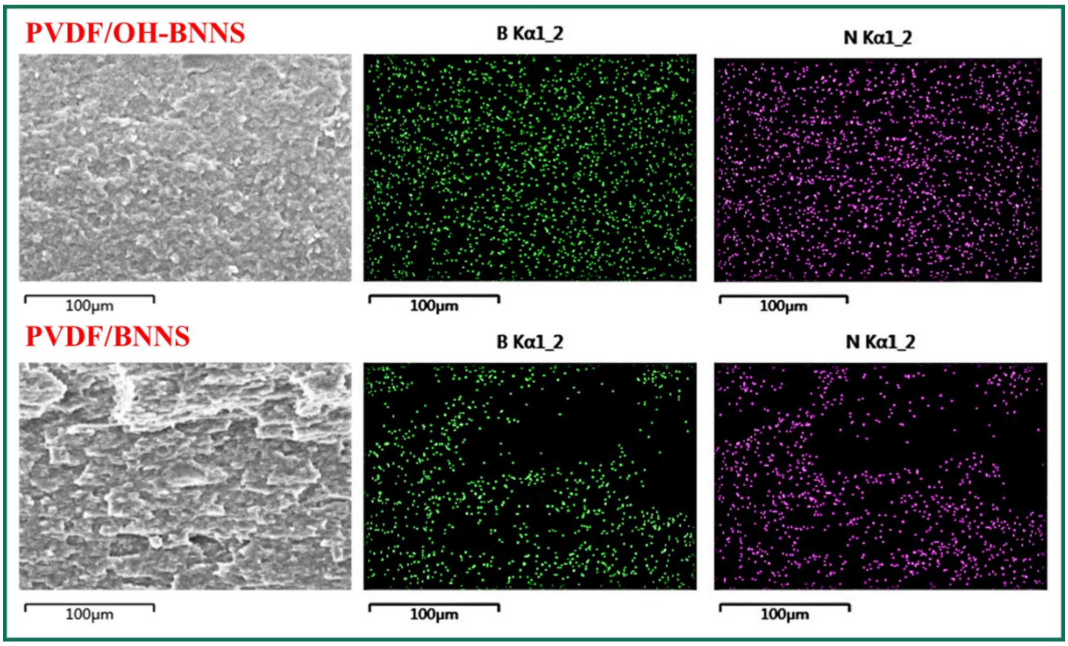

Fig. S4 STEM analysis and EDX element mapping of PVDF/BNNS and PVDF/OH-BNNS nanocomposites, respectively.

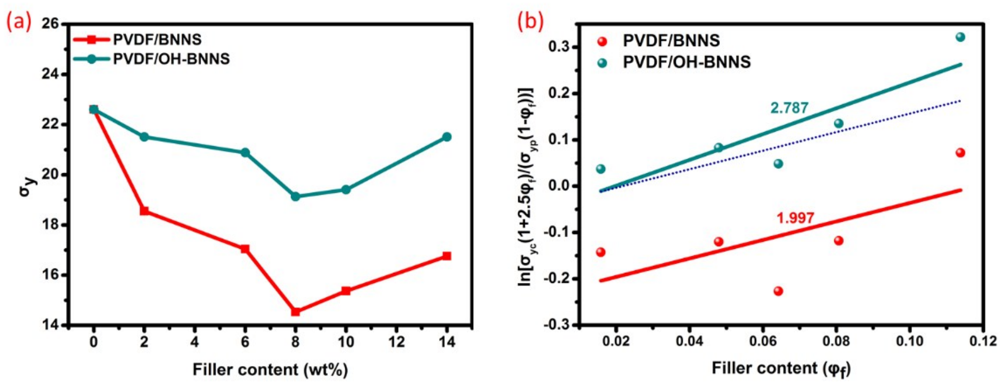

Fig. S5 (a) Yield stress and (b) interfacial interactivity parameter B of the PVDF/BNNS and PVDF/OH-BNNS nanocomposites. And lines in (b) were obtained by linear fitting in origin. The interfacial interaction can be evaluated by a semiempirical equation: $\sigma_{yc} = \frac{1 - \Phi_f}{1 + 2.5\Phi_f} exp(B\Phi_f)$. Where σ_{yc} and σ_{yp} are yield stress of the nanocomposite and polymer matrix, respectively, while Φ_f is the volume fraction of filler, and B is a parameter which indicates the interfacial interaction in the nanocomposites. If

$ln[\sigma_{yc}(1+2.5\Phi_f)/(\sigma_{yp}(1-\Phi_f))]$ of fraction value is plotted against Φ_f of BNNSs and OH-BNNSs dispersed phase, parameter B can be calculated as a line slope. This assumes the σ_{yc} to be constant. And the values of interfacial interaction parameter B, evaluated from σ_y values are 2.787 and 1.997 for PVDF/OH-BNNS and PVDF/BNNS nanocomposites, respectively.

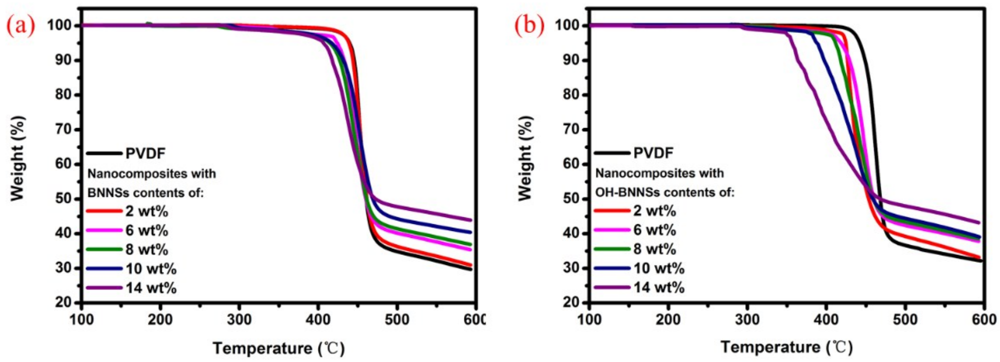

Fig. S6 TGA curves of (a) PVDF/BNNS and (b) PVDF/OH-BNNS nanocomposites.

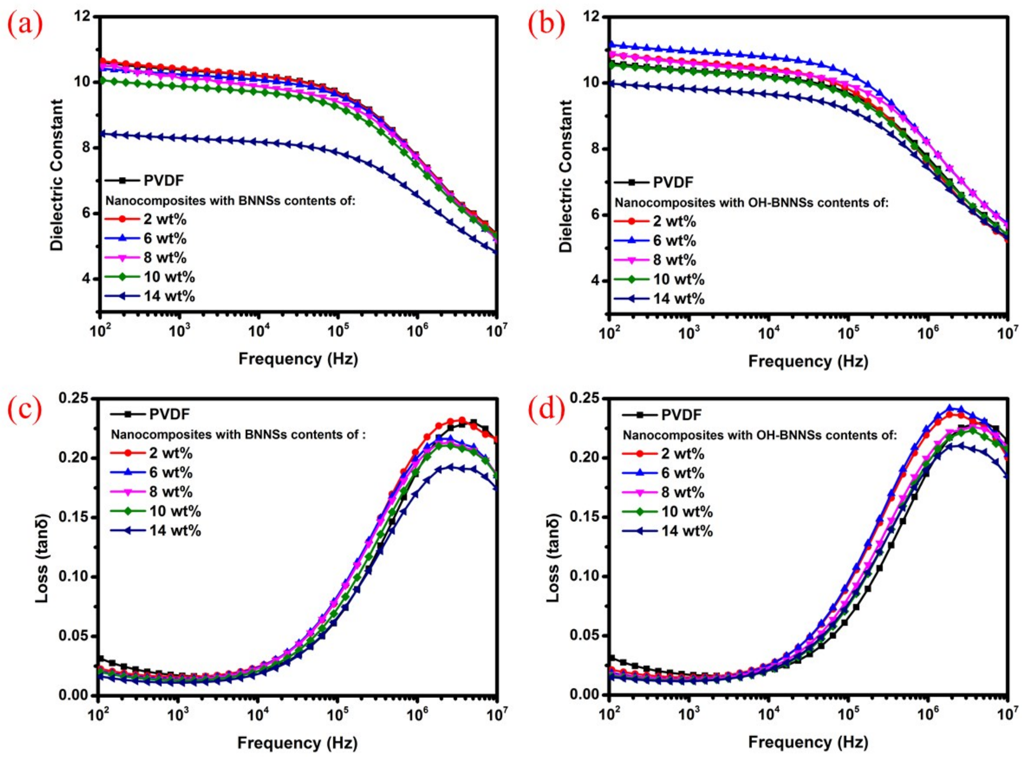

Fig. S7 Frequency dependence of the dielectric constant of (a) PVDF/BNNS and (b) PVDF/OH-BNNS nanocomposites, respectively. Frequency dependence of the dielectric loss tangent (c) PVDF/BNNS and (d) PVDF/OH-BNNS nanocomposites.

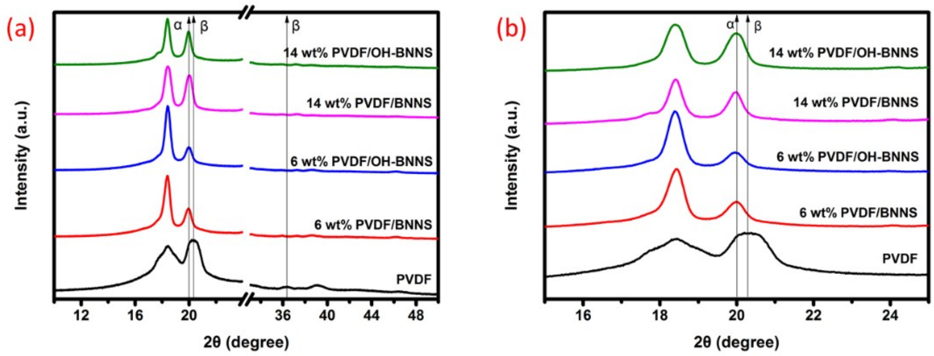

Fig. S8 (a) XRD histogram of the PVDF, 6 wt% PVDF/BNNS, 6 wt% PVDF/OH-BNNS, 14 wt% PVDF/BNNS and 14 wt% PVDF/OH-BNNS samples; (b) enlarged view of XRD histogram (15–25°) of these samples.

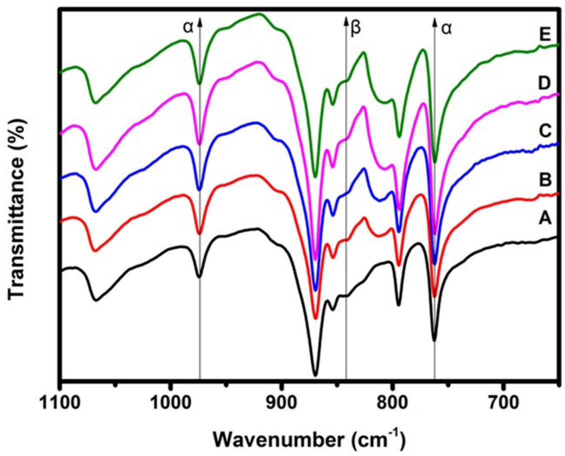

Fig. S9 The FTIR spectra of A. PVDF, B. 6 wt% PVDF/BNNS, C. 6 wt% PVDF/OH-BNNS, D. 14 wt% PVDF/BNNS and E. 14 wt% PVDF/OH-BNNS samples.

Table S1. The thermal diffusivity, density and specific heat capacity of PVDF-based nanocomposites.

Sample	α // (mm^2/s)	ρ (g/cm^3)	C (kJ/kg K)
Neat PVDF	1.26	1.77	1.2
2 wt% BNNS	1.967	1.771	1.19
6 wt% BNNS	2.383	1.792	1.171
8 wt% BNNS	2.464	1.802	1.161
10 wt% BNNS	2.555	1.813	1.151

14 wt% BNNS	2.881	1.834	1.131
2 wt% OH-BNNS	2.452	1.771	1.190
6 wt% OH-BNNS	2.994	1.792	1.171
8 wt% OH-BNNS	3.206	1.802	1.161
10 wt% OH-BNNS	3.435	1.813	1.151
14 wt% OH-BNNS	3.66	1.834	1.131

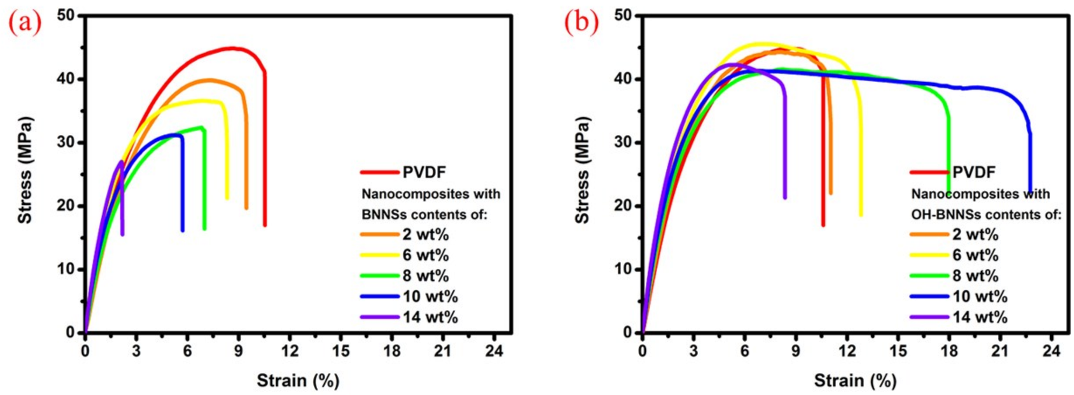

Fig. S10 The stress-strain curves of (a) PVDF/BNNS nanocomposites and (b) PVDF/OH-BNNS nanocomposites.

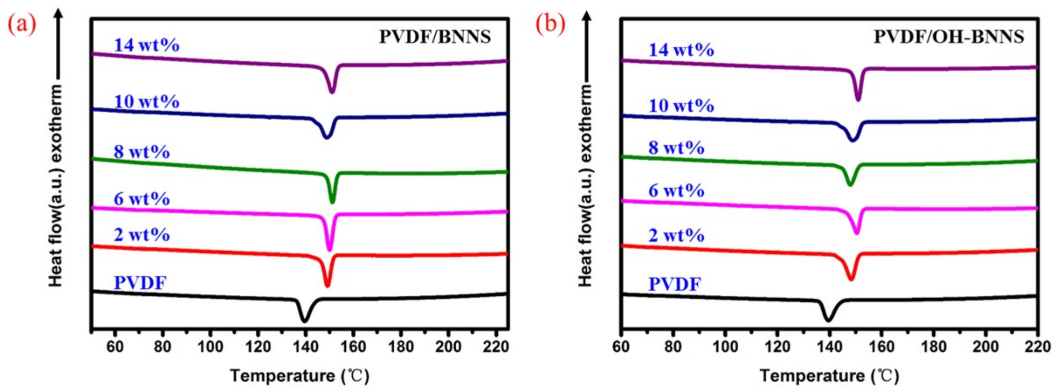

Fig. S11 DSC curves of (a) PVDF/BNNS and (b) PVDF/OH-BNNS nanocomposites during the heating cycle.

Table S2. Crystallization temperature and crystallinity of the crystalline domain of PVDF-based nanocomposites.

Sample	T_c(℃)	Crystallinity (%)
Neat PVDF	132.720	44.59

2 wt% BNNS	154.922	44.53
6 wt% BNNS	154.125	40.52
8 wt% BNNS	151.195	37.69
10 wt% BNNS	148.862	43.51
14 wt% BNNS	151.190	43.90
2 wt% OH-BNNS	147.808	43.85
6 wt% OH-BNNS	150.526	41.38
8 wt% OH-BNNS	148.020	43.46
10 wt% OH-BNNS	150.698	42.66
14 wt% OH-BNNS	151.015	40.95